UDC 621.396.969.029.6:004.942

V. VOLOSYUK, S. ZHYLA, V. PAVLIKOV, E. TSERNE,
A. SOBKOLOV, O. SHMATKO, K. BELOUSOV

National Aerospace University "Kharkiv Aviation Institute", Ukraine

MATHEMATICAL DESCRIPTION OF IMAGING PROCESSES IN ULTRA-WIDEBAND ACTIVE APERTURE SYNTHESIS SYSTEMS USING STOCHASTIC SOUNDING SIGNALS

Mathematical models of the fields of stochastic ultra-wideband signals that are necessary for solving problems of aperture synthesis of images using active radar methods are presented. The expediency of using V-transformations in these problems has been substantiated, the effectiveness of which has already been proven for the mathematical description of ultra-wideband spatio-temporal fields in the methods of passive and active radar, as well as remote sensing, that are used to solve problems of radio astronomy, medicine, navigation. Using modern methods of mathematical analysis and the theory of ultra-wideband systems, the physical essence of radio images obtained with the help of algorithms for coherent and incoherent signal processing is investigated. According to these algorithms, it is proposed to divide images into coherent and incoherent. Coherent images include those in which its amplitude and phase are recorded separately. In the case of an incoherent image, only its amplitude (power or related characteristic) is recorded. To describe of the obtained radio image structure, new concepts of the spectral density of the complex spatial coherence function (SDCSCF) and the spectral density of the spatial autocorrelation function of the amplitude-phase distribution (SDFSAF APD) are introduced. Application-use of functions is expedient and fundamentally necessary for solving problems of aperture synthesis using stochastic ultra-wideband signals. A mathematical description of the structures obtained by aperture synthesis of radio images is given. Here, studies are conducted for the general case of using a continuous (idealized) aperture, and for using an antenna system with spatially separated receiving elements. Simulation of the heuristic synthesized algorithm for constructing incoherent radio images is conducted. The possibility of using antenna arrays and synthesized aperture synthesis algorithms for solving problems of image formation in a survey located directly under the aircraft (at sounding angles close to vertical) are substantiated.

Keywords: active aperture synthesis; radar imaging; V-transforms.

Introduction

Motivation. State of the Art. Aerospace radar systems with synthetic aperture are typically used for surface imaging in significantly lateral directions relative to their flight trajectory (±20°...50° from the direction to the nadir). This is due to the possibility of providing the required range resolution within these directions by using short probing impulses or pulses with good correlation properties (for example, impulses with linear-frequency (LFM) or phase modulation (PM)). The resolution of coherent and incoherent side-looking airborne radar is absent directly under the aircraft, over the coordinate perpendicular to the direction of its movement (in the nadir) [1-3].

The problem of imaging directly under the aircraft can be solved by using underwing or ventral antenna arrays, which are a part of multifunctional radar systems, in combination with wide- and ultra-wideband signal processing. In this case, it is expedient to use stochastic processes in the form of wide- or ultra-wideband Gaussian noise as the probing signals. This will provide narrow single-lobe uncertainty functions with low sidelobe levels and allows the application of methods of spatial [4-6] and spectral aperture image synthesis [7-9] used in radio astronomy [10, 11]. Since the aperture synthesis over time narrows the uncertainty function only along the movement trajectory and does not influence the lateral direction, we will neglect the effect of velocity when solving this problem.

It should be noted that modern advances in radio electronics allow using of aperture synthesis methods in combination with wideband and ultra-wideband signals. Modern radioelements make it possible to form and process ultra-wide-width noise signals, such digital processing devices as FPGAs in combination with high-speed ADCs allow flexible implementation of the necessary algorithms for the operation of wideband radars in digital form.

Objectives. This article continues researches [12-14] and proposes the development of a method for the formation of incoherent and coherent radio images for the systems of active aperture synthesis.

Purpose of the article. Development and research of an algorithm for radio images formation of the underlying surface from an aerospace carrier by ultra-wideband aperture synthesis systems at sounding angles close to nadir.

Initial data, preliminary reasoning and problem statement

Let us obtain the initial data and clarify the problem statement for imaging method development by analyzing geometry of the problem. One of the possible geometries, which can explain the process of forming an image for the investigated surface, is shown in Fig. 1.
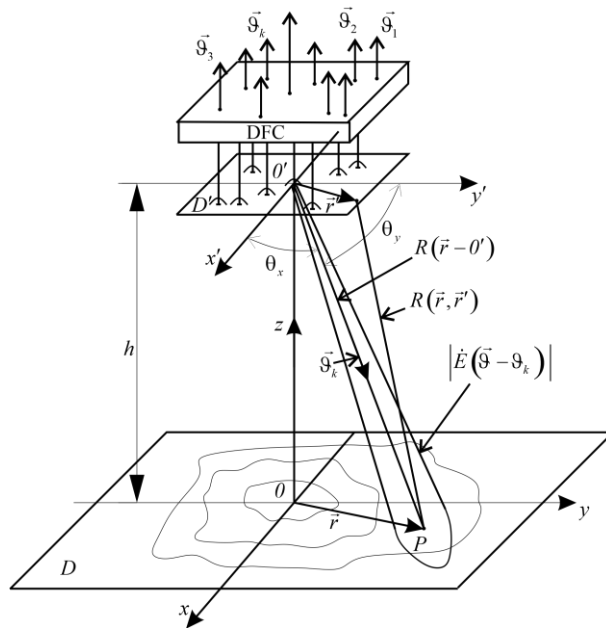

Fig. 1. Image formation in an active aperture synthesis system

We introduce the following notions in Fig. 1: $x \, y \, z$ represent a coordinate system connected with the underlying surface; $x' \, y' \, h$ is a coordinate system associated with the phase center of the receiving antenna system; D' is the observation area; D is the underlying surface area; $\vec{r}$ is a radius vector characterizing the reflective point position on the underlying surface; $\vec{r}'$ is the radius vector characterizing the position of the observation point in the area D'; $R(\vec{r} - 0')$ is the distance from an emitting point $0'$ to a surface element $d\vec{r}$ with its center in the point P; $R(\vec{r}, \vec{r}')$ is the distance from the surface element $d\vec{r}$ with its center in the point P to the observation point in the observation area D'; θ_x, θ_y are the angles between axels x', y' and the

direction to the surface element $d\vec{r}$ with its center in the point P; $\left| \dot{E}(\vec{9} - \vec{9}_k) \right|$ is a module of the antenna system radiation pattern focused in the direction $\vec{9}_k$.

The position of the underlying surface points is characterized by the end of the radius vector $\vec{r} = (x, y, z)$; points within the range of emission and reception – by the end of the radius vector $\vec{r}' = (x', y', h)$.

It is expedient to represent the probing signal $s(t)$ in the form of Gaussian random process segments with zero mathematical expectation $\langle s(t) \rangle = 0$ (hereinafter, the brackets $\langle \cdot \rangle$ denote the statistical averaging operator). Let us use the spectral representation of the signal over its spectral density of the complex amplitude $\dot{S}(j2\pi f)$

$$s(t) = \int_{-\infty}^{\infty} \dot{S}(j2\pi f) \exp(j2f\,t) dt, \; \langle \dot{S}(j2\pi f) \rangle = 0, \; (1)$$

where f are the temporal frequencies, t is time.

Signal (1) is emitted by the transmitting antenna of the radio system, the phase center of which is aligned with the point $0'$ of the coordinate system origin $\vec{r}' = (x', y')$, arising from the observation area $\vec{r}' \in D'$. This signal irradiates the investigated surface D, reflects from all elementary areas $d\vec{r}$ with their coordinates $\vec{r} \in D$, and is received in the observation area D'. Coefficient of signal reflection from elements of the surface $d\vec{r}$ we represent by a statistically inhomogeneous function of angular coordinates (direction cosines $\vec{9} = (9_x = \cos\theta_x, 9_y = \cos\theta_y)$)

$$\dot{F}(\vec{r}(\vec{9}), f) = \dot{F}(\vec{9}, f). \qquad (2)$$

This complex function plays an important role in solving the problems of imaging, since it contains the amplitude and phase information about the reflective properties of the studied object's surface. It can be referred to as a coherent image [13-15].

We'd assume that the area D' consist elements of the receiving antenna system with an amplitude-phase distribution (APD) of their receiving sensitivity $\dot{I}(f, \vec{r}')$. In the simplest case, when an equal-amplitude in-phase aperture is considered, we write $\dot{I}(f, \vec{r}') = 1$, $\vec{r}' \in D'$.

When focusing the antenna system in a certain direction characterized by the k-th vector of the direction

cosines $\vec{\vartheta}_k$, we represent APD at each frequency f as the following function:

$$\dot{I}\left(f, \vec{r}', \vec{\vartheta}_k\right) = \exp\left(-j2\pi f\, c^{-1}\vec{\vartheta}_k \vec{r}'\right) = \exp\left(-jk\,\vec{\vartheta}_k \vec{r}'\right),$$
$$\vec{r}' \in D', \tag{3}$$

where $k = 2\pi f/c = 2\pi/\lambda$ is the wave number (a function of frequency in the case of using wideband signals), λ is the wavelength.

For most of the imaging problems, the following condition is fulfilled: the dimensions of the antenna system are much less than the distance to the surface. This allows us to assume that the objects of observation are located in the Fraunhofer zone.

The distance, which the waves pass from the radiation point $0'$ to the surface element $d\vec{r}$ centered at the point P (the position of which is characterized by the end of the radius vector $\vec{r}$) and back to the point of observation (characterized by the end of the radius vector $\vec{r}'$), we write in the following way:

$$R\left(\vec{r}(\vec{\vartheta}), \vec{r}'\right) \approx 2R\left(\vec{r}, 0'\right) - \vec{\vartheta}\vec{r}', \tag{4}$$

where $\vec{\vartheta}\vec{r}' = \vartheta_x x' + \vartheta_y y'$ is the scalar product of vectors.

The resulting field in the elementary observation area is characterized by the end of the radius vector $\vec{r}' = (x', y', h)$ and can be represented as a superposition of the fields formed by every element of the reflecting surface at each of the frequencies

$$s\left(\vec{r}', t\right) \approx \int_{-\infty}^{\infty} \int_{-\infty}^{\infty} \frac{\dot{S}\left(j2\pi f\right)}{R^2\left(\vec{r}, 0'\right)} \dot{F}\left(\vec{\vartheta}, f\right) \dot{I}\left(\vec{r}', f\right) \times$$
$$\times \exp\left(j2\pi f\left(t - 2c^{-1}R\left(\vec{r}, 0'\right) + c^{-1}\vec{\vartheta}\vec{r}'\right)\right) df d\vec{\vartheta}, \tag{5}$$

where denominator $R^2\left(\vec{r}, 0'\right)$ describes attenuation of the signal amplitude during its propagation.

Direct estimation of the coherent image $\dot{F}\left(\vec{\vartheta}, f\right)$ is a rather difficult task. This is due to the difficulty of controlling the phase at the distance $R\left(\vec{r}, 0'\right)$. It is much easier to estimate the amplitude changes of the function $\dot{F}\left(\vec{\vartheta}, f\right)$. Therefore, the phase factor containing the phase incursion at the distance $R\left(\vec{r}, 0'\right)$ can be excluded from consideration or, formally, can be considered included in the function $\dot{F}(\vec{\vartheta}, f)$. The attenuation

multiplier $R^{-2}\left(\vec{r}, 0'\right)$ as a proportionality coefficient can also be neglected (considered included in the function $\dot{F}(\vec{\vartheta}, f)$).

In addition, we can assume that each elementary section of the receiving antenna system limited by the area D' can be characterized by its own APD, thus sampling over the receiving area will be performed at the final stage of the signal processing algorithm interpretation. This way, (5) is formally reduced to the mathematical apparatus of V- transforms [16-18]

$$s\left(\vec{r}', t\right) = V_F^{-1}\left\{\dot{S}_F\left(\vec{\vartheta}, f\right)\right\} = \int_{-\infty}^{\infty} \int_{-\infty}^{\infty} \dot{S}_F\left(\vec{\vartheta}, f\right) \times$$
$$\times \exp\left(j2\pi f\left(t + c^{-1}\vec{\vartheta}\vec{r}'\right)\right) df d\vec{\vartheta},$$

$$f^{-2}c^2 \dot{S}_F\left(\vec{\vartheta}, f\right) = V_F\left\{s\left(\vec{r}', t\right)\right\} = \int_{-\infty}^{+\infty} \int s\left(\vec{r}', t\right) \times$$
$$\times \exp\left(-j2\pi f\left(t + c^{-1}\vec{\vartheta}\vec{r}'\right)\right) dt d\vec{r}', \tag{6}$$

where the following notations are introduced:

$$\dot{S}_F\left(\vec{\vartheta}, f\right) = \dot{S}\left(j2\pi f\right) \dot{F}\left(\vec{\vartheta}, f\right) \dot{I}\left(\vec{r}', f\right), \tag{7}$$

$V_F\left\{\cdot\right\}$ and $V_F^{-1}\left\{\cdot\right\}$ are the operator forms of direct and indirect V_F transform. The main feature of practical implementation of these transforms lies in their applicability for working with ultra-wideband signals and no requirement in fulfilling the conditions of quasi-monochromatic approximation (QMA) [12] (space-time narrowband-ness (STN) [13]), which consist in neglecting the delay of the complex envelope for the spatio-temporal signal even at the most extreme points of the antenna system aperture – that is typical in case of narrowband signal processing.

This way we established the connection between the spatio-temporal signal $s\left(\vec{r}', t\right)$ in the observation area and the function $\dot{S}_F\left(\vec{\vartheta}, f\right)$ over a pair of V_F- transforms, and showed how the coherent radio image is contained in the spatio-temporal signal observed by the elements of the receiving antenna.

In such a case, the problem statement can be formulated as follows. On the basis of the known sample for a wideband spatio-temporal field $s\left(\vec{r}', t\right)$ we must develop an algorithm for the formation of a coherent radio image $\dot{S}_F\left(\vec{\vartheta}, f\right)$ or $\dot{F}\left(\vec{\vartheta}, f\right)$ in the registration area (which is limited by the receiving antenna). Here, it

should be noted that it is rather difficult to restore a coherent image using a radio system, thus in most practical cases it is expedient to restore an incoherent image. Therefore, we shall correct the problem statement to the following form: "on the basis of the known sample for a wideband spatio-temporal field $s(\vec{r}',t)$ we must develop an algorithm for the incoherent radio image formation in the registration area (limited by the receiving antenna)." In order to do so, let us clarify the physical essence of an incoherent image and establish its connection with a coherent image.

Correlation of incoherent and coherent images

Let us show the connection between coherent and incoherent images.

It is known that the property of uncorrelated spectral densities of complex amplitudes for different frequencies is fulfilled for stationary random processes:

$$\left\langle \dot{S}\left(j2\pi f_1\right)\dot{S}^*\left(j2\pi f_2\right)\right\rangle = G\left(f_1\right)\delta\left(f_1 - f_2\right), \qquad (8)$$

where $G(f)$ is the energy spectrum (spectral power density (SPD)) of a random process $s(t)$, $\delta(f_1 - f_2)$ is the delta-function. We can also assume that mathematical expectation of the complex scattering coefficient is equal to zero, i.e. $\left\langle \dot{F}\left[\vartheta(\vec{r})\right]\right\rangle = 0$, and its values for arbitrary non-coinciding surface elements are uncorrelated:

$$\left\langle \dot{F}\left(\vartheta_1(\vec{r}_1)\right)\dot{F}^*\left(\vartheta_2(\vec{r}_2)\right)\right\rangle = \sigma^0\left(\vec{\vartheta}_1, f\right)\delta\left(\vec{\vartheta}_1 - \vec{\vartheta}_2\right). \quad (9)$$

This condition is fulfilled for surfaces covered with fine-structured irregularities, dimensions of which exceed the wavelength (arable land, shrubs, grass, etc.). Here, $\sigma^0\left(\vec{\vartheta}, f\right)$ is a specific effective backscattering cross-section [1, 16] (specific effective scattering surface (ESS)) of the surface element $d\vec{r}$ observed in the direction $\vec{\vartheta}$. This function is proportional to the wave reflection coefficient over power, and will be further considered as the true desired incoherent image of the surface.

Based on the above, it is clear that the incoherent image is contained not in the spatio-temporal field observed in the area of the receiving antenna, but in its statistical characteristic – the function of spatial correlation (coherence).

Development of an algorithm for incoherent image formation. New definitions and their correlation with radio images received by wideband radio systems

In order to solve the problem of passive remote sensing, we have established connection between the correlation function of the process and the radio image on the basis of a pair of V_F - transforms on the basis of methodology [18-21].

$$R(\Delta\vec{r}', \tau) = \left\langle s(\vec{r}_1', t_1)s(\vec{r}_2', t_2)\right\rangle = V_F^{-1}\left\{G_\sigma\left(\vec{\vartheta}, f\right)\right\} =$$

$$= \int\limits_{-\infty}^{\infty}\int\limits_{-\infty}^{\infty} G_\sigma\left(\vec{\vartheta}, f\right)\exp\left(j2\pi f\left(\tau + c^{-1}\,\vec{\vartheta}\,\Delta\vec{r}'\right)\right)df\,d\vec{\vartheta} \ ,(10)$$

$$f^{-2}c^2 G_\sigma\left(\vec{\vartheta}, f\right) = V_F\left\{R\left(\Delta\vec{r}', \tau\right)\right\} =$$

$$= \int\limits_{-\infty}^{\infty}\int\limits_{-\infty}^{\infty} R\left(\Delta\vec{r}', \tau\right)\exp\left(-j2\pi f\left(\tau + c^{-1}\vec{\vartheta}\,\Delta\vec{r}'\right)\right)d\tau d\Delta\vec{r}' \ .(11)$$

Here, $R(\Delta\vec{r}', \tau)$ is the correlation function of a stationary and homogeneous process $s(\vec{r}', t)$, $\Delta\vec{r}' = \vec{r}_1' - \vec{r}_2'$, $\tau = t_1 - t_2$,

$$G_\sigma\left(\vec{\vartheta}, f\right) = G(f)\sigma^0\left(\vec{\vartheta}, f\right). \qquad (12)$$

Since SPD of the probe signal $G(f)$ is known, and the function $G_\sigma\left(\vec{\vartheta}, f\right)$ can be divided into it, it is expedient to consider product (12) as the desired incoherent image of the surface at each specific frequency.

The obtained expressions describe the fields and their characteristics within the observation area D' that is free from antenna devices. The presence of receiving antenna elements we take into account by introducing APD $\dot{I}(\vec{r}', f)$ into the observation area. In the simplest case, an image of a spatially extended object can be obtained in the parallel view mode by simultaneously focusing the antenna system on various directions $\vec{\vartheta}_i$ covering the object with APD in the form of (3), or by scanning an object with APD over time:

$$\dot{I}\left(f, \vec{r}', \vec{\vartheta}(t)\right) = \exp\left(-jk\,\vec{\vartheta}(t)\vec{r}'\right), \ \vec{r}' \in D'. \quad (13)$$

The focusing process, which lies in the in-phase addition of all spectral components of the received signal, is usually performed by a diagram-forming circuit (DFC) (Fig. 1). The in-phase-ness of the signals re-

ceived by individual elements of the antenna system via appropriate phase delays, provides APD in the form of (3), (13). In general, for ultra-wideband signals, it is provided by the time delays that correspond to the sloping front of the received spatio-temporal signal. In modern narrowband systems, the function of DFC can be performed by a computing device after the formation of complex envelopes for the received signals and their subsequent digitization. The figure above represents an example of the radio imaging system and the primary stage of image aperture synthesis at the level of its coherent description. In case of a parallel view, each direction $\vec{\vartheta}_k$ at the output of DFC corresponds to its own output. The received signal at each of such outputs with the APD in the form of (3) can be represented by the following expression:

$$
s\left(t, \vec{\vartheta}_k\right) = \int\limits_{-\infty(\Theta)}^{\infty} \int\limits_{-\infty(F)}^{\infty} \int\limits_{-\infty(D')}^{\infty} \dot{K}(j2\pi f)\dot{I}\left(f, \vec{r}', \vec{\vartheta}_k\right)\dot{S}_F\left(\vec{\vartheta}, f\right)\times
$$

$$
\times \exp\left(j2\pi\left(t + \frac{\vec{\vartheta}\,\vec{r}'}{c} \right) \right) d\vec{r}' df\, d\vec{\vartheta} = \int\limits_{-\infty(F)}^{\infty} \int\limits_{-\infty(\Theta)}^{\infty} \dot{K}\left(j2\pi f\right)\times
$$

$$
\times \dot{E}\left(f, \vec{\vartheta} - \vec{\vartheta}_k\right)\dot{S}_F\left(\vec{\vartheta}, f\right)\exp\left(j2\pi f\, t\right)df\, d\vec{\vartheta} \quad (14)
$$

where $\dot{E}\left(f, \vec{\vartheta} - \vec{\vartheta}_k\right)$ is the antenna pattern (AP) of each partial beam of the antenna system (for an antenna array (AA) this is its multiplier); $\dot{K}(j\,2\pi f)$ is the transmission coefficient for the aperture element $d\vec{r}'$ (assumed identical for all elements of the aperture D' and all outputs of the DFC). For the real discrete AA these are transmission coefficients of primary receiving devices connected to the outputs of individual elementary antennas included in the AA. Antenna patterns of the beams are correlated with the respective APD by the spatial Fourier transforms

$$
\dot{E}\left(f, \vec{\vartheta} - \vec{\vartheta}_k\right) = \mathcal{F}^{-1}_{\vec{r}' \to \vec{\vartheta}}\left\{\dot{I}\left(f, \vec{r}', \vec{\vartheta}_k\right)\right\} =
$$

$$
= \int\limits_{-\infty(D')}^{\infty} \dot{I}\left(f, \vec{r}', \vec{\vartheta}_k\right)\exp\left(j2\pi f\, \vec{\vartheta}\, \frac{\vec{r}'}{c} \right)d\vec{r}', \quad (15)
$$

$$
\dot{I}\left(f, \vec{r}', \vec{\vartheta}_k\right) = \left(\frac{f}{c}\right)^2 \mathcal{F}_{\vec{\vartheta} \to \vec{r}'}\left\{\dot{E}\left(f, \vec{\vartheta} - \vec{\vartheta}_k\right)\right\} =
$$

$$
= \int\limits_{-\infty(D')}^{\infty} \dot{E}\left(f, \vec{\vartheta} - \vec{\vartheta}_k\right)\exp\left(-j2\pi f\, \frac{\vec{\vartheta}\, \vec{r}'}{c} \right)d\vec{r}' \quad (16)
$$

where $\mathcal{F}_{x \to y}\{\cdot\}$ are the spatial Fourier transforms from one set of variables to the respective set of others.

Function $s\left(t, \vec{\vartheta}_k\right)$ defined by expression (14) is real, since it is the Fourier transform of the corresponding spectral density of the complex amplitude within symmetric limits $f \in (-\infty, \infty)$. As a function of angular coordinates, it can be considered as an estimate of the image. An estimate of a quantity is an approximate realization obtained as a result of the measurements. However, estimate (13) has a random nature; it changes over time and is not suitable for visualization. A more appropriate image estimate is the average power of this signal $\hat{P}_{av}\left(\vec{\vartheta}_k\right)$, which, in accordance with the statistical averaging procedure, is the variance $\sigma_s^2\left(\vartheta_k\right)$ of a random process $s\left(t, \vec{\vartheta}_k\right)$. Average signal power is often referred to as the signal intensity $\hat{I}\left(\vec{\vartheta}_k\right)$. These values are proportional to the integral (over frequencies) values of the specific ESS. The sign ^ denotes image estimation.

Estimate $\hat{P}_{av}\left(\vec{\vartheta}_k\right)$ can be defined in the following way:

$$
\hat{P}_{av}\left(\vec{\vartheta}_k\right) = \left\langle s^2\left(t, \vec{\vartheta}_k\right)\right\rangle = \sigma_s^2\left(\vartheta_k\right) = \hat{I}\left(\vec{\vartheta}_k\right) =
$$

$$
= \int\limits_{-\infty(D')}^{\infty} \int\limits_{-\infty(D')}^{\infty} \int\limits_{-\infty(\Theta)}^{\infty} \int\limits_{-\infty(\Theta)}^{\infty} \int\limits_{-\infty(F)}^{\infty} \int\limits_{-\infty(F)}^{\infty} \dot{K}(j2\pi f_1)\times
$$

$$
\times \dot{K}^*(j2\pi f_2)\times \dot{I}\left(f_1, \vec{r}_1', \vec{\vartheta}_k\right)\dot{I}^*\left(f_2, \vec{r}_2', \vec{\vartheta}_k\right)\times
$$

$$
\times \left\langle \dot{S}(f_1)\dot{S}^*(f_2)\right\rangle\left\langle \dot{F}\left(\vec{\vartheta}_1\left(\vec{r}_1\right)\right)\dot{F}^*\left(\vec{\vartheta}_2\left(\vec{r}_2\right)\right)\right\rangle\times
$$

$$
\times \exp\left(j2\pi(f_1 - f_2)\, t\right)\times \exp\left(j2\pi\left(f_1\frac{\vec{\vartheta}_2\, \vec{r}_1'}{c} - \right.\right.
$$

$$
\left.\left. -f_2\frac{\vec{\vartheta}_3\, \vec{r}_2'}{c} \right)\right)df_1\, df_2\, d\vec{\vartheta}_2\, d\vec{\vartheta}_3\, d\vec{r}_1' d\vec{r}_2'.
$$

Taking into account (8) and (9), we get

$$
\hat{I}\left(\vec{\vartheta}_k\right) = \int\limits_{-\infty(F)}^{\infty} \int\limits_{-\infty(\Theta)}^{\infty} \left|\dot{K}(j2\pi f)\right|^2 \left|\dot{E}\left(f, \vec{\vartheta} - \vec{\vartheta}_k\right)\right|^2 \times
$$

$$
\times G_\sigma\left(\vec{\vartheta}, f\right)d\vec{\vartheta} df = \int\limits_{-\infty(F)}^{\infty} \left|\dot{K}(j2\pi f)\right|^2 G_{\hat{\sigma}}\left(\vec{\vartheta}_k, f\right)df, \quad (17)
$$

where $G_{\hat{\sigma}}\left(f, \vec{\vartheta}_k\right)$ is the energy spectrum of a random signal at the output of the k-th DFC channel focused on one of the directions $\vec{\vartheta}_k$. It can be considered up to a factor $G(f)$ as an estimate of the specific ESS $\sigma^0\left(\vec{\vartheta}_k, f\right)$, i.e.

$$G_{\hat{\sigma}}\left(\vec{\vartheta}_k, f\right) = \int\limits_{-\infty(\Theta)}^{\infty} \left|\dot{F}\left(f, \vec{\vartheta}-\vec{\vartheta}_k\right)\right|^2 G_{\sigma}\left(\vec{\vartheta}, f\right) d\vec{\vartheta} =$$

$$= G(f) \int\limits_{-\infty(\Theta)}^{\infty} \left|\dot{F}\left(f, \vec{\vartheta}-\vec{\vartheta}_k\right)\right|^2 \sigma^0\left(\vec{\vartheta}, f\right) d\vec{\vartheta}. \quad (18)$$

Here, $G_{\hat{\sigma}}\left(\vec{\vartheta}, f\right)$ is the estimate of the function $G_{\sigma}\left(\vec{\vartheta}, f\right)$, and $\hat{\sigma}^0\left(\vec{\vartheta}, f\right) = G_{\hat{\sigma}}\left(\vec{\vartheta}, f\right)/G(f)$ is the estimate of the specific ESS at each specific frequency, which at this frequency is considered as an incoherent energy image of the surface. This image is smoothed (defocused) by the AP $\left|\dot{E}\left(f, \vec{\vartheta}-\vec{\vartheta}_k\right)\right|^2$, which at each frequency of the ultra-wideband signal is a hardware function of the sensing system determining resolution of the incoherent imaging system. The quality of resolution for individual image elements as a whole is determined by the shape of AP $\dot{E}\left(f, \vec{\vartheta}-\vec{\vartheta}_k\right)$ at various frequencies f, the spectrum width $\dot{S}(j2\pi f)$ of the emitted signal, and the bandwidth within the transfer characteristic $\dot{K}(j2\pi f)$.

According to the obtained expression, the imaging algorithm $\hat{I}\left(\vec{\vartheta}_k\right)$ must contain the operations of focusing the antenna system on a variety of directions $\vec{\vartheta}_k$ and measuring the corresponding powers of fluctuations received from these directions.

Let us present these formulas in a different form, introducing the concepts of the spectral density for the spatial coherence complex function and the spectral density of the APD autocorrelation function.

Spectral densities of the complex spatial coherence function and the autocorrelation function of the APD

Let us consider $V_F^{-1}\{\cdot\}$ transform (10) for the spectral function of incoherent image $G_{\sigma}\left(\vec{\vartheta}, f\right)$ into the correlation function $R\left(\tau, \Delta\vec{r}'\right)$

$$R\left(\tau, \Delta\vec{r}'\right) = V_F^{-1}\left\{G_{\sigma}\left(\vec{\vartheta}, f\right)\right\} = \int\limits_{-\infty}^{\infty}\int\limits_{-\infty}^{\infty} G_{\sigma}\left(\vec{\vartheta}, f\right) \times$$

$$\times \exp\left(j2\pi f\left(\tau + \frac{\vec{\vartheta}\,\Delta\vec{r}'}{c}\right)\right) df\, d\vec{\vartheta} = \int\limits_{-\infty(F)}^{\infty} \exp\left(j2\pi f\,\tau\right) \times$$

$$\times \int\limits_{-\infty(\Theta)}^{\infty} G_{\sigma}\left(\vec{\vartheta}, f\right) \exp\left(j2\pi f\,\frac{\vec{\vartheta}\,\Delta\vec{r}'}{c}\right) d\vec{\vartheta}\, df =$$

$$= \int\limits_{-\infty(F)}^{\infty} \dot{\Gamma}_{\sigma}\left(f, \Delta\vec{r}'\right) \exp\left(j2\pi f\,\tau\right) df. \quad (19)$$

Function

$$\dot{\Gamma}_{\sigma}\left(f, \Delta\vec{r}'\right) = \mathcal{F}_{\vec{\vartheta}\to\Delta\vec{r}'}^{-1}\left\{G_{\sigma}\left(\vec{\vartheta}, f\right)\right\} =$$

$$= \mathcal{F}_{\tau\to f}\left\{R\left(\tau, \Delta\vec{r}'\right)\right\}, \quad (20)$$

in contrast to the classical complex spatial coherence function of a narrowband signal, which satisfies the QMA condition [12], when using a stochastic ultrawideband signal the spectral density of the complex spatial coherence function (SDCSCF) at the frequency f makes a valid sense.

This function can be found by applying the inverse spatial Fourier transform to the spectral function of the image $G_{\sigma}\left(\vec{\vartheta}, f\right)$.

$$\dot{\Gamma}_{\sigma}\left(f, \Delta\vec{r}'\right) = \mathcal{F}_{\vec{\vartheta}\to\Delta\vec{r}'}^{-1}\left\{G_{\sigma}\left(\vec{\vartheta}, f\right)\right\} =$$

$$= \int\limits_{-\infty(\Theta)}^{\infty} G_{\sigma}\left(\vec{\vartheta}, f\right) \exp\left(j2\pi f\,\frac{\vec{\vartheta}\,\Delta\vec{r}'}{c}\right) d\vec{\vartheta}, \quad (21)$$

$$\frac{c^2}{f^2} G_{\sigma}\left(\vec{\vartheta}, f\right) = \mathcal{F}_{\Delta\vec{r}'\to\vec{\vartheta}}\left\{\dot{\Gamma}_{\sigma}\left(f, \Delta\vec{r}'\right)\right\} =$$

$$= \int\limits_{-\infty(D')}^{\infty} \dot{\Gamma}_{\sigma}\left(f, \Delta\vec{r}'\right) \exp\left(-j2\pi f\,\frac{\vec{\vartheta}\,\Delta\vec{r}'}{c}\right) d\Delta\vec{r}', \quad (22)$$

and by the temporal variable of the direct Fourier transform applied to the autocorrelation function $R\left(\tau, \Delta\vec{r}'\right)$,

$$\dot{\Gamma}_{\sigma}\left(f, \Delta\vec{r}'\right) = \mathcal{F}_{\tau\to f}\left\{R\left(\tau, \Delta\vec{r}'\right)\right\} =$$

$$= \int\limits_{-\infty(\tau)}^{\infty} R\left(\tau, \Delta\vec{r}'\right) \exp\left(-j2\pi f\tau\right) d\tau, \quad (23)$$

$$R\left(\tau, \Delta\vec{r}'\right) = \mathcal{F}_{f\to\tau}^{-1}\left\{\dot{\Gamma}_{\sigma}\left(f, \Delta\vec{r}'\right)\right\} =$$

$$= \int\limits_{-\infty(F)}^{\infty} \dot{\Gamma}_{\sigma}\left(f, \Delta\vec{r}'\right) \exp\left(j2\pi f\tau\right) df, \quad (24)$$

Spectral image function $G_{\sigma}\left(\vec{\vartheta}, f\right)$ at each specific frequency f is real, and the complex function $\dot{\Gamma}_{\sigma}\left(f, \Delta\vec{r}'\right)$ represents its spatial spectrum. In problems

of radio astronomy, this spectrum is determined as a function of spatial frequencies $\Delta\vec{r}'_\lambda = f\,\Delta\vec{r}'/c = \Delta\vec{r}'/\lambda$.

In contrast to narrow-band systems, for which we use the concept of the spatial autocorrelation function of APD, correlates with the central frequency of the signal spectrum or the receiving system frequency band, we can introduce the concept of the spectral density for the spatial autocorrelation function of APD (SDFSAF APD)

$$\dot{R}_{APD}\left(f,\Delta\vec{r}',\vec{\vartheta}_k\right) = \int\limits_{-\infty(D')}^{\infty} \dot{I}\left(f,\vec{r}',\vec{\vartheta}_k\right)\times$$

$$\times \dot{I}^*\left(f,\vec{r}'-\Delta\vec{r}',\vec{\vartheta}_k\right) d\vec{r}'. \qquad (25)$$

We apply the Fourier transform to the square of the AP modules.

As a result, we get

$$\mathcal{F}_{\vec{\vartheta}\to\Delta\vec{r}'}\left\{\left|\dot{E}\left(f,\vec{\vartheta}-\vec{\vartheta}_k\right)\right|^2\right\} =$$

$$= \left(\frac{c}{f}\right)^2 \dot{R}_{A\Phi P}\left(f,\,\Delta\vec{r}',\vec{\vartheta}_k\right). \qquad (26)$$

Obviously, the reverse transform is also valid:

$$\left|\dot{E}\left(f,\vec{\vartheta}-\vec{\vartheta}_k\right)\right|^2 = \mathcal{F}^{-1}_{\Delta\vec{r}'\to\vec{\vartheta}}\left\{\dot{R}_{APD}\left(f,\Delta\vec{r}',\vec{\vartheta}_k\right)\right\}. \quad (27)$$

Thus, the squared module of AP and the spectral density of the spatial autocorrelation function of APD are related to each other by a pair of spatial Fourier transforms.

In the considered case of active sensing of the surface by stochastic signals, when registering the spatial spectral components of the spectral image function $G_\sigma\left(\vec{\vartheta},f\right)$, SDFSAF APD at each individual frequency f is considered as the spatio-spectral transfer characteristic of the antenna system. In radio astronomy, for narrowband signals with their central frequency f_0, the autocorrelation function of the APD is often considered as a function of spatial frequencies $\Delta\vec{r}'_\lambda = \Delta\vec{r}'/\lambda_0$

$$\dot{R}_{APD}\left(f_0,\Delta\vec{r}'_\lambda,\vec{\vartheta}_k\right) = \int\limits_{-\infty(D')}^{\infty} \dot{I}\left(f,\vec{r}'_\lambda,\vec{\vartheta}_k\right)\times$$

$$\times\dot{I}^*\left(f,\vec{r}'_\lambda-\Delta\vec{r}'_\lambda,\vec{\vartheta}_k\right)d\vec{r}'_\lambda, \qquad (28)$$

and is referred to as the spatio-spectral function of antenna sensitivity. The spectral density of the spatial coherence function and the spectral density of the APD autocorrelation function are consistent with the classical theory of Fourier transforms over time as the spectral densities for complex amplitudes. Unlike narrowband

signals, which are used in radio astronomy for passive systems when receiving the intrinsic radiation of objects with their functions attributed to the central carrier frequency, for ultra-wideband signals used in both active and passive systems these functions should be assigned to each specific frequency of their temporal spectrums.

Mathematical relationship of image estimation with SDCSCF and SDFSAF APD

Estimates of images (17), (18), which contain the functions $G_\sigma\left(\vec{\vartheta},f\right)$ and $\left|\dot{E}\left(f,\vec{\vartheta}-\vec{\vartheta}_k\right)\right|^2$, can be expressed via their corresponding spectral characteristics SDCSCF $\dot{\Gamma}_\sigma\left(f,\Delta\vec{r}'\right)$ and SDFSAF APD $\dot{R}_{APD}\left(f,\Delta\vec{r}',\vec{\vartheta}_k\right)$. Let us substitute the functions $G_\sigma\left(\vec{\vartheta},f\right)$ and $\left|\dot{E}\left(f,\vec{\vartheta}-\vec{\vartheta}_i\right)\right|^2$ in the form of their corresponding Fourier transforms (22,27) from SDCSCF and SDFSAF APD in these formulas. This way the image estimate (17) can be represented by the following equivalent expressions:

$$\hat{I}\left(\vec{\vartheta}_k\right) = \int\limits_{-\infty(F)}^{\infty}\left|\dot{K}(j2\pi f)\right|^2 \int\limits_{-\infty(\Theta)}^{\infty}\left|\dot{E}\left(f,\vec{\vartheta}-\vec{\vartheta}_k\right)\right|^2\times$$

$$\times G_\sigma\left(\vec{\vartheta},f\right)d\vec{\vartheta}\,df = \int\limits_{-\infty(F)}^{\infty}\left|\dot{K}(j2\pi f)\right|^2\times$$

$$\times \int\limits_{D'(\Delta\vec{r}',-\infty)}^{\infty}\dot{R}_{APD}\left(f,\Delta\vec{r}',\vec{\vartheta}_k\right)\dot{\Gamma}_\sigma\left(f,\Delta\vec{r}'\right)d\Delta\vec{r}'\,df. \quad (29)$$

Since the integral

$$G_{\hat{\sigma}}\left(\vec{\vartheta},f\right) = \int\limits_{-\infty(\Theta)}^{\infty}\left|\dot{E}\left(f,\vec{\vartheta}-\vec{\vartheta}_k\right)\right|^2 G_\sigma\left(\vec{\vartheta},f\right)d\vec{\vartheta} \quad (30)$$

is real at each frequency f, the integral below will be real as well:

$$G_{\hat{\sigma}}\left(\vec{\vartheta}_k,f\right) = \int\limits_{D'(\Delta\vec{r}',-\infty)}^{\infty}\dot{R}_{APD}\left(f,\Delta\vec{r}',\vec{\vartheta}_k\right)\times$$

$$\times\dot{\Gamma}_\sigma\left(f,\Delta\vec{r}'\right)d\Delta\vec{r}'. \qquad (31)$$

Functions $\dot{R}_{APD}\left(f,\Delta\vec{r}',\vec{\vartheta}_k\right)$ and $\dot{\Gamma}_\sigma\left(f,\Delta\vec{r}'\right)$ respectively are the complex spatial Fourier images (spectrums) of the functions $\left|\dot{E}\left(f,\vec{\vartheta}-\vec{\vartheta}_k\right)\right|^2$ and $G_\sigma\left(\vec{\vartheta},f\right)$. Therefore, function $\dot{\Gamma}_\sigma\left(f,\Delta\vec{r}'\right)$ is the spatial spectrum

of the image, when $\dot{R}_{APD}\left(f,\Delta\vec{r}',\vec{\vartheta}_k\right)$ is the complex spatial transmission coefficient of the antenna system characterizing its ability to transmit the harmonics of various spatial frequencies included in the image.

Formula (29) indicates a possible physical sequence of actions, as a result of which the estimate $\hat{I}\left(\vec{\vartheta}_k\right)$ is formed. This sequence consists in the formation of a complex correlation function (coherence function) at a given frequency f and its multiplication by the APD autocorrelation function at the same frequency f. In order to form the image (29) as a corresponding dependence of the average power, it is necessary to integrate the estimates of the spectral functions (30) or (31) over the selected frequency band specified by the transmission coefficient $\dot{K}(j2\pi f)$.

In the above formulas, the autocorrelation function of the APD is presented in general form. Let us consider some of the possible useful options for specifying this function. A useful concretization of this function is based on the concept of an idealized continuous aperture with the ability to control APD at each of its points, for example, by introducing a phase delay function to each of its points (3). Then the APD of such an aperture can be represented by the following expression:

$$\dot{I}\left(f,\vec{r}',\vec{\vartheta}_k\right)=\dot{I}_{basic}\left(f,\vec{r}'\right)\exp\left(-j2\pi f\frac{\vec{\vartheta}_k\vec{r}'}{c}\right). \quad (32)$$

Here $\dot{I}_{basic}\left(f,\vec{r}'\right)$ is the initial (basic) APD of the continual aperture, at each point of which there is a possibility of independent change in amplitude and phase of the incident field. In the simplest case,

$$\dot{I}_{basic}\left(f,\vec{r}'\right)=\begin{cases}1 & \text{при }\vec{r}'\in D';\\0 & \text{при }\vec{r}'\notin D'.\end{cases} \quad (33)$$

In many cases, as opposed to discrete apertures, the use of a continuous aperture simplifies the mathematical analysis of antenna systems using well-known integral transforms (Fourier, Fresnel, etc.) At the final stages of research, the transition from continuous to discrete apertures is carried out using the appropriate discretization of the obtained expressions. It should be noted that in antenna arrays (AA) consisting of a discrete set of identical elementary antennas the function $\dot{E}\left(f_1,\vec{\vartheta}-\vec{\vartheta}_k\right)$ is referred to as its factor, the co-factor of which is the AP of the elementary antenna. These APs as the co-factors can be formally associated with each point of the continuous antenna.

APD of the real AA can be described as follows:

$$\dot{I}\left(f,\vec{r}',\vec{\vartheta}_k\right)=\sum_{i=1}^{N}\dot{I}_{ai}\left(f,\vec{r}'-\vec{r}_i'\right)\exp\left(-j2\pi f\frac{\vec{\vartheta}_k\vec{r}_i'}{c}\right). \quad (34)$$

In this case, elementary antennas with the basic APD $\dot{I}_{ai}\left(f,\vec{r}'-\vec{r}_i'\right)$, $i=\overline{1,N}$ are located in the aperture area D'. We assume that when focusing the AA on the direction $\vec{\vartheta}_i$, the phase shifts are introduced only at the outputs of elementary antennas. Here, the exponential factors correspond to the transfer coefficients of the devices used to align the phases of oscillations received from the direction $\vec{\vartheta}_k$ over individual elements of the AA with its phase centers $\vec{r}_i'$. Regardless of the AA geometry, we chose sequential numbering for the antennas in order to simplify the resulting formula. The focusing of the antennas on the direction $\vec{\vartheta}_k$ is provided by in-phase summation of the delayed signals taken from the outputs of the elementary antennas at each frequency. The multiplier $\exp\left(-j2\pi f\,\vec{\vartheta}_k\,\vec{r}_i'\,c^{-1}\right)$ is the transmission coefficient for the delay line of the received signal over the time $\vec{\vartheta}_k\,\vec{r}_i'c^{-1}$. This is a transmission coefficient of the phase shifter at each individual frequency f.

To begin with, we find SDFSAF APD for the continuous idealized APD (32):

$$\dot{R}_{APD}\left(f,\Delta\vec{r}',\vec{\vartheta}_k\right)=\int\limits_{-\infty(D')}^{\infty}\dot{I}\left(f,\vec{r}',\vec{\vartheta}_k\right)\times$$

$$\times\dot{I}^{*}\left(f,\vec{r}'-\Delta\vec{r}',\vec{\vartheta}_k\right)d\vec{r}'=\exp\left(-j2\pi f\frac{\vec{\vartheta}_k\Delta\vec{r}'}{c}\right)\times$$

$$\times\int\limits_{-\infty(D')}^{\infty}\dot{I}_{basik}\left(f,\vec{r}'\right)\dot{I}_{basik}^{*}\left(f,\vec{r}'-\Delta\vec{r}'\right)d\vec{r}'=$$

$$=\dot{R}_{basik(APD)}\left(f,\Delta\vec{r}'\right)\exp\left(-j2\pi f\frac{\vec{\vartheta}_k\Delta\vec{r}'}{c}\right). \quad (35)$$

As a result, mathematical structure of the image (29) will take the following form:

$$\hat{I}\left(\vec{\vartheta}_k\right)=\int\limits_{-\infty(\Delta\vec{r}',D')}^{\infty}\int\limits_{-\infty(F)}^{\infty}\left|\dot{K}(j2\pi f)\right|^{2}\times$$

$$\times\dot{R}_{APD}\left(f,\Delta\vec{r}',\vec{\vartheta}_k\right)\dot{\Gamma}_{\sigma}\left(f,\Delta\vec{r}'\right)df\,d\Delta\vec{r}'=$$

$$=\int\limits_{-\infty(F)}^{\infty}\left|\dot{K}(j2\pi f)\right|^{2}\times\int\limits_{-\infty(\Delta\vec{r}',D')}^{\infty}\dot{R}_{basik(APD)}\left(f,\Delta\vec{r}'\right)\times$$

$$\times\dot{\Gamma}_{\sigma}\left(f,\Delta\vec{r}'\right)\exp\left(-j2\pi f\frac{\vec{\vartheta}_k\Delta\vec{r}'}{c}\right)d\Delta\vec{r}'df\,, \quad (36)$$

where

$$\dot{R}_{basik(APD)}(f,\Delta\vec{r}') =$$

$$= \int\limits_{-\infty(D')}^{\infty} \dot{I}_{basik}(f,\vec{r}')\dot{I}_{basik}^{*}(f,\vec{r}'-\Delta\vec{r}')\,d\vec{r}' \quad (37)$$

is the SDCSCF of the basic continual APD.

Comparing the resulting image with formula (17), we can see that here the inner integral is an estimate of the spectral function of the image $G_{\sigma}(\vec{\vartheta},f)$, which can be represented in the form of the following three integrals

$$G_{\hat{\sigma}}(\vec{\vartheta}_k,f) = \int\limits_{-\infty(\Theta)}^{\infty} \left|\dot{E}(f,\vec{\vartheta}-\vec{\vartheta}_k)\right|^2 \times$$

$$\times G_{\sigma}(\vec{\vartheta},f)\,d\vec{\vartheta} = \int\limits_{-\infty(\Delta\vec{r}',D')}^{\infty} \dot{R}_{APD}(f,\Delta\vec{r}',\vec{\vartheta}_k) \times$$

$$\times \dot{\Gamma}_{\sigma}(f,\Delta\vec{r}')\,df\,d\Delta\vec{r}' = \int\limits_{-\infty(\Delta\vec{r}',D')}^{\infty} \dot{R}_{basik(APD)}(f,\Delta\vec{r}') \times$$

$$\times \dot{\Gamma}_{\sigma}(f,\Delta\vec{r}')\exp\left(-j2\pi f\frac{\vec{\vartheta}_k\,\Delta\vec{r}'}{c}\right)d\Delta\vec{r}'. \quad (38)$$

In the second integral (38), the functions $\dot{R}_{APD}(f,\Delta\vec{r}',\vec{\vartheta}_k)$ and $\dot{\Gamma}_{\sigma}(f,\Delta\vec{r}')$ are the spatial spectrums of the integrands in the first integral. The physical meaning of the third integral is as follows. The RBI estimate at each separate frequency is found as the spatial Fourier image of the product of SDCSCF $\dot{\Gamma}_{\sigma}(f,\Delta\vec{r}')$ for the field observed within the aperture of the antenna system and the SDFSAF $\dot{R}_{basik(APD)}(f,\Delta\vec{r}')$ of the basic continuous APD.

In the idealized case of an infinite aperture $\dot{R}_{basik(APD)}(f,\Delta\vec{r}') = const$, we obtain formulas (19) - (24). If we consider function $\dot{\Gamma}_{\sigma}(f,\Delta\vec{r}')$ as a spatial spectrum of the spectral brightness $G_{\sigma}(\vec{\vartheta},f)$, the function $\dot{R}_{basik(APD)}(f,\Delta\vec{r}')$ will be considered as the spatial complex transmission coefficient of the antenna system with regard to this spectrum. It is important for this coefficient and, respectively, the entire antenna system to provide registration of the maximum number of harmonics within the spatial spectrum of spectral brightness $G_{\sigma}(\vec{\vartheta},f)$. This estimate is separate for each frequency f. Therefore, such an estimate should be expected to be close to the image estimate for a narrowband signal at the center frequency f_0, which satisfies the QMA condition.

In the second, real in practical terms option of receiving signals by an antenna array with APD (34) SDFSAF APD will take the next form:

$$\dot{R}_{APD}(f,\Delta\vec{r}',\vec{\vartheta}_k) = \sum_{i=1}^{N}\sum_{n=1}^{N} \dot{R}_{ain(APD)}(f,\Delta\vec{r}'-(\vec{r}_i'-\vec{r}_n')) \times$$

$$\times\exp\left(-j2\pi f\frac{\vec{\vartheta}_k(\vec{r}_i'-\vec{r}_n')}{c}\right), \quad (39)$$

In this case, we get the following mathematical structure for evaluating the image (29):

$$\hat{I}(\vec{\vartheta}_k) = \int\limits_{-\infty(F)}^{\infty} \left|\dot{K}(j2\pi f)\right|^2 \times$$

$$\times\sum_{i=1}^{N}\sum_{n=1}^{N}\dot{\Gamma}_{in}(f)\exp\left(-j2\pi f\frac{\vec{\vartheta}_k(\vec{r}_i'-\vec{r}_n')}{c}\right)df, \quad (40)$$

where

$$\dot{R}_{ain(APD)}\left[f,\Delta\vec{r}'-(\vec{r}_i'-\vec{r}_n')\right] =$$

$$= \int\limits_{-\infty(D')}^{\infty} \dot{I}_{ai}(f,\vec{r}'-\vec{r}_i')\,\dot{I}_{an}(f,\vec{r}'-\Delta\vec{r}'-\vec{r}_n')\,d\vec{r}', \quad (41)$$

and the spectral densities of the spatial cross-correlation functions of the basic APDs for elementary antennas of the AA can be determined by the expression

$$\dot{\Gamma}_{in}(f) = \int\limits_{-\infty(\Delta\vec{r}',D')}^{\infty} \dot{R}_{ain(APD)}(f,\Delta\vec{r}'-(\vec{r}_i'-\vec{r}_n')) \times$$

$$\times\dot{\Gamma}_{\sigma}(f,\Delta\vec{r}')d\Delta\vec{r}' = \int\limits_{-\infty(\Delta\vec{r}',D')}^{\infty}\int\limits_{-\infty(D')}^{\infty} \dot{I}_{ai}(f,\vec{r}'-\vec{r}_i') \times$$

$$\times\dot{I}_{an}^{*}(f,\vec{r}'-\Delta\vec{r}'-\vec{r}_n') \times \int\limits_{-\infty(\Theta)}^{\infty} G_{\sigma}(\vec{\vartheta},f) \times$$

$$\times\exp\left(j2\pi f\frac{\vec{\vartheta}\,\Delta\vec{r}'}{c}\right)d\vec{\vartheta}d\vec{r}'d\Delta\vec{r}' =$$

$$= \left|\vec{r}'=\vec{r}_1',\ \vec{r}'-\Delta\vec{r}'=\vec{r}_2',\ \Delta\vec{r}'=\vec{r}_1'-\vec{r}_2'\right| =$$

$$= \int\limits_{-\infty(D')}^{\infty}\int\limits_{-\infty(D')}^{\infty} \dot{I}_{ai}(f,\vec{r}_1'-\vec{r}_i')\dot{I}_{an}^{*}(f,\vec{r}_2'-\vec{r}_n') \times$$

$$\times \int\limits_{-\infty(\Theta)}^{\infty} G_{\sigma}(\vec{\vartheta},f)\exp\left(j2\pi f\frac{\vec{\vartheta}(\vec{r}_1'-\vec{r}_2')}{c}\right)d\vec{\vartheta}d\vec{r}_1'd\vec{r}_2', \quad (42)$$

By performing transition to the Fourier images of the integrands, we obtain

$$\dot{\Gamma}_{in}(f) = \int\limits_{-\infty(\Theta)}^{\infty} \dot{E}_{ai}(f,\vec{\vartheta})\dot{E}_{an}^{*}(f,\vec{\vartheta}) \times$$

$$\times G_{\sigma}(\vec{\vartheta},f)\exp\left(j2\pi f\vec{\vartheta}\frac{(\vec{r}_i' - \vec{r}_n')}{c}\right)d\vec{\vartheta}, \qquad (43)$$

The final expression for evaluating an incoherent image $\hat{I}(\vec{\vartheta}_k)$ in the AA with its APD (34) can be written as follows:

$$\hat{I}(\vec{\vartheta}_k) = \int\limits_{-\infty(F)}^{\infty} \left|\dot{K}(j2\pi f)\right|^2 \times$$

$$\times \int\limits_{-\infty(\Theta)}^{\infty} \left|\dot{E}(f,\vec{\vartheta}-\vec{\vartheta}_k)\right|^2 \times G_{\sigma}(\vec{\vartheta},f)d\vec{\vartheta}df =$$

$$= \int\limits_{-\infty(F)}^{\infty} \left|\dot{K}(j2\pi f)\right|^2 \int\limits_{-\infty(\Delta\vec{r}',D')}^{\infty} \dot{R}_{APD}(f,\Delta\vec{r}',\vec{\vartheta}_k) \times$$

$$\times\dot{\Gamma}_{\sigma}(f,\Delta\vec{r}')d\Delta\vec{r}'df = \int\limits_{-\infty(F)}^{\infty} \left|\dot{K}(j2\pi f)\right|^2 \sum_{i=1}^{N}\sum_{n=1}^{N}\dot{\Gamma}_{in}(f) \times$$

$$\times\exp\left(-j2\pi f\frac{\vec{\vartheta}_k(\vec{r}_i'-\vec{r}_n')}{c}\right)df = \int\limits_{-\infty(F)}^{\infty} \left|\dot{K}(j2\pi f)\right|^2 \times$$

$$\times\sum_{i=1}^{N}\sum_{n=1}^{N}\left\{\int\limits_{-\infty(\Delta\vec{r}',D')}^{\infty} \dot{R}_{ain(APD)}(f,\Delta\vec{r}'-(\vec{r}_i-\vec{r}_n)) \times \atop \times G_{\sigma}(f,\Delta\vec{r}')d\Delta\vec{r}'\right\} \times$$

$$\times\exp\left(-j2\pi f\frac{\vec{\vartheta}_1(\vec{r}_i'-\vec{r}_n')}{c}\right)df = \int\limits_{-\infty(F)}^{\infty} \left|\dot{K}(j2\pi f)\right|^2 \times$$

$$\times\sum_{i=1}^{N}\sum_{n=1}^{N}\left\{\int\limits_{-\infty(\Theta)}^{\infty} \dot{E}_{ai}(f,\vec{\vartheta})\dot{E}_{an}^{*}(f,\vec{\vartheta})G_{\sigma}(f,\vec{\vartheta}) \times \atop \times\exp\left(j2\pi f\vec{\vartheta}\frac{(\vec{r}_i'-\vec{r}_k')}{c}\right)d\vec{\vartheta}\right\} \times$$

$$\times\exp\left(-j2\pi f\frac{\vec{\vartheta}_1(\vec{r}_i'-\vec{r}_k')}{c}\right)df. \qquad (44)$$

According to the last version of formula (44), the imaging process in the AA can be represented by the following mathematical operations:

1) a set of numbers $\dot{\Gamma}_{in}(f)$ is formed at each frequency f, which is the result of integration over $\Delta\vec{r}'$ for the product of spectral density of the spatial coherence function $\dot{\Gamma}_{\sigma}(f,\Delta\vec{r}')$, and the spectral densities of spatial cross-correlation functions for the basic APD $\dot{R}_{ain(APD)}(f,\Delta\vec{r}'-(\vec{r}_i-\vec{r}_n))$ of the elementary antennas,

which form the antenna array;

2) a discrete Fourier transform is applied to the resulting set of numbers

$$\sum_{i=1}^{N}\sum_{n=1}^{N}\dot{\Gamma}_{in}(f)\exp\left(-j2\pi f\frac{\vec{\vartheta}_k\Delta\vec{r}_{in}'}{c}\right),$$

$$\Delta\vec{r}_{in}' = \vec{r}_i' - \vec{r}_n';$$

3) the obtained result is integrated over each frequency f.

Simulation results

Let us perform the formation of a radar image using the signal processing algorithm (44).

Let the receiving antenna system have the form shown in the Fig. 2. The emitting antenna is located at the center of the antenna system. The antenna array has a square shape, consists of 25 antennas, the distance between the phase centers of neighboring elements is 0.8 m. The diameter of each antenna is 0.1 m.
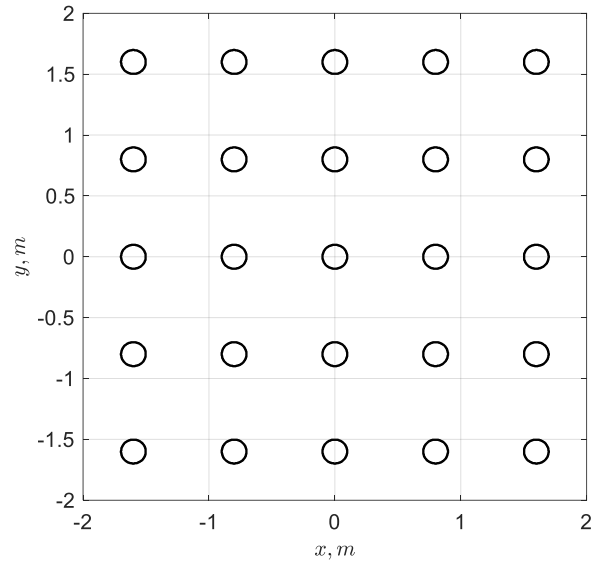
Fig. 2. Receiving antenna array geometry

The simulation is carried out for a range of frequencies of the probing signal 50-70 GHz, which corresponds to the capabilities of a modern radioelement base. Thus, modern amplifiers [22-24], mixers [25], single antennas and antenna arrays [26-28], digital signal processing devices [29, 30] allow processing ultra-wideband signals.

In accordance with the algorithm (44), in order to obtain the primary radio image, it is initially necessary to calculate the spectral density of the spatial cross-

correlation functions of the basic APD $\dot{R}_{ain(APD)}\left(f,\Delta\vec{r}'-\left(\vec{r}_i-\vec{r}_n\right)\right)$. It is obtained as a result of the Fourier transform of the cross-correlation function of the basic APD for the elements of a receiving antenna array. The cross-correlation function of the basic APD is shown in the Figure 3.
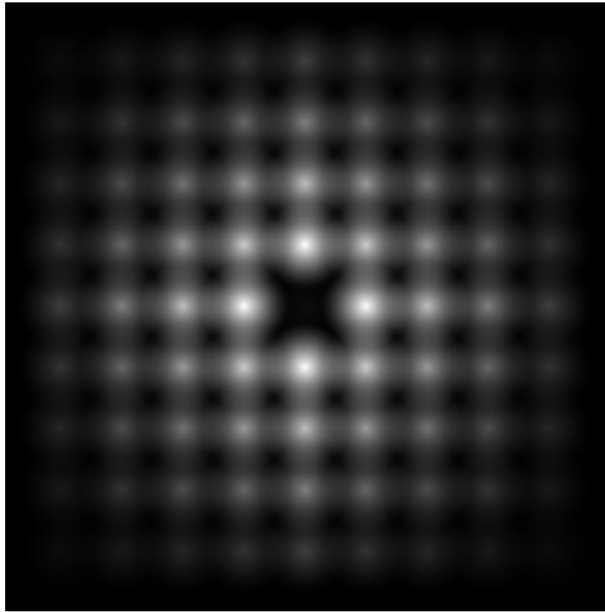

Fig. 3. Cross-correlation function of basic APD of elementary antennas of AA

The Fourier transform of the test image is used as the spectral density of the spatial coherence function $\dot{\Gamma}_\sigma\left(f,\Delta\vec{r}'\right)$. The test image is shown in the Figure 4.

Fig. 4. Test image

Further, the multiplication of $\dot{R}_{ain(APD)}\left(f,\Delta\vec{r}'-\left(\vec{r}_i-\vec{r}_n\right)\right)$ and $\dot{\Gamma}_\sigma\left(f,\Delta\vec{r}'\right)$ is performed, and the resulting product is integrated over $\Delta\vec{r}'$. The inverse Fourier transform was applied to the result of integration, and the result of the transformation is averaged over all frequencies. As a result, a primary radiometric image is obtained. It's shown in the Figure 5.

The resulting primary radio image is similar to the derivative of the test image. This is due to the periodic form of the cross-correlation function of the basic AFR. Despite this in the primary radar image, individual objects can be easily distinguished by visual analysis. the quality of the image shown in Figure 3, b can be significantly improved in the process of its secondary processing [31-33] (for example, by neural networks, decorrelating filter or other types of filters using [34-36]).
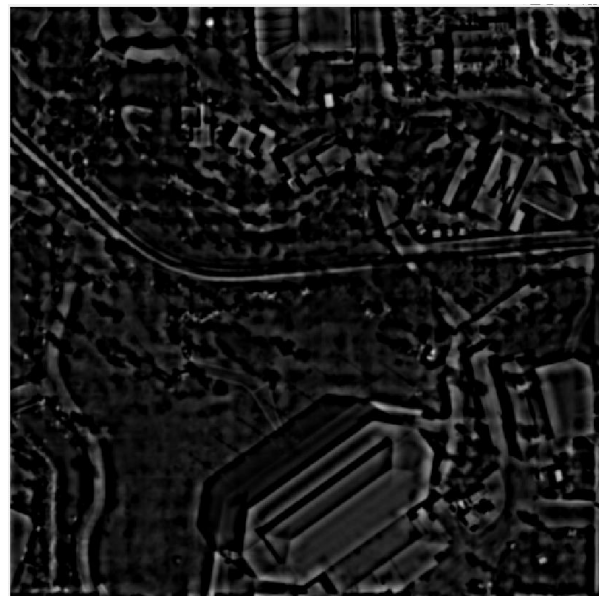

Fig. 5. Primary radiometric image

Conclusions

To solve the problems of image aperture synthesis via active remote sensing systems using stochastic ultra-wideband signals, the mathematical structure of coherent and incoherent surface images was considered and investigated. In particular, we have considered the problem of surface imaging directly under the aircraft in the dead zone, where conventional synthetic aperture radars cannot provide the necessary resolution in the lateral directions relative to the direction of their movement. To provide an adequate description of the image structure, we introduced the new concepts for spectral density of the spatial coherence function and the spectral

density of the APD autocorrelation function, the use of which is expedient when probing surfaces with stochastic ultra-wideband signals and solving problems of the corresponding aperture synthesis.

It is shown that an estimate of the incoherent image synthesized based on stochastic ultra-wideband signal contains, in one particular case, mathematical operations of convolution for the effective scattering cross-section with an array multiplier and integration over the frequencies, the weight of which corresponds to the probing signal spectrum. In the second case, the equivalent sequence of actions contains the operations of spatial Fourier transform for the product of the spatial coherence function spectral density with the spectral density of the APD correlation function and the similar integration over the corresponding frequency band. The mathematical structure of the image was considered in its general form, in the specific form for the idealized continuous aperture, and the aperture of a real antenna array.

As a part of future research, a model that implements the operation of the algorithm (44) will be created, and practical results regarding the application of this algorithm in practice will be obtained.

References (GOST 7.1:2006)

1. A new method of multi-frequency active aperture synthesis for imaging of SAR blind zone under aerospace vehicle [Text] / V. Pavlikov, V. Volosyuk, S. Zhyla, H. N. Van, K. N. Van // 2017 14th International Conference The Experience of Designing and Application of CAD Systems in Microelectronics. CADSM. – Polyana, 2017. – P 118-120. DOI: 10.1109/CADSM.2017.7916099.

2. Villano, M. Nadir Echo Removal in Synthetic Aperture Radar via Waveform Diversity and Dual-Focus Postprocessing [Text] / M. Villano, G. Krieger, A. Moreira // IEEE Geoscience and Remote Sensing Letters. – 2018. – Vol. 15, no. 5. – P. 719-723. DOI: 10.1109/LGRS.2018.2808196

3. Torres, R. Overview of Copernicus SAR Space Component and its Evolution [Text] / R. Torres, M. Davidson // 2019 IEEE International Geoscience and Remote Sensing Symposium. IGARSS 2019. – Yokohama, 2019. – P. 5381-5384. DOI: 10.1109/IGARSS.2019.8899134

4. Morrison, R. L. Radio Astronomy Techniques for Multistatic Radar Imaging and Localization of Space Objects [Text] / R. L Morrison, E. B. Phelps //

2019 International Applied Computational Electromagnetics Society Symposium. ACES. – Miami, 2019. – P. 1-2.

5. Wei, L. Robust recovery for aperture synthesis imaging [Text] / L. Wei, S. J. Wijnholds, P. Hurley // 2017 IEEE International Conference on Image Processing. ICIP. – Beijing, 2017. – P. 3570-3574. DOI: 10.1109/ICIP.2017.8296947.

6. Methods of multiposition radar aperture synthesis [Text] / I. A. Kuzmin, Z. V. Merkulova, A. Y. Sheremet, T. A. Dovgal, V. V. Chistukhin // 2017 IEEE Conference of Russian Young Researchers in Electrical and Electronic Engineering. EIConRus. – Moscow, 2017. – P. 1247-1248. DOI: 10.1109/EIConRus.2017.7910789.

7. Pavlikov, V. V. Spectral method for the spatio-spectral sensitivity domain filling in aperture synthesis system [Text] / V. V. Pavlikov, N. V. Kiem, O. M. Tymoschuk // 2016 8th International Conference on Ultrawideband and Ultrashort Impulse Signals. UWBUSIS. – Odessa, 2016. – P. 124-127. DOI: 10.1109/UWBUSIS.2016.7724167.

8. Inverse aperture synthesis in the intermediate zone of radiation for radio image forming by optimal filtration with evolutionary control [Text] / O. O. Drobakhin, G. G. Sherstyuk, A. G. Mamedov, A. Y. Tuluk // 2016 8th International Conference on Ultrawideband and Ultrashort Impulse Signals. UWBUSIS. – Odessa, 2016. – P. 109-111. DOI: 10.1109/UWBUSIS.2016.7724163.

9. The Maximum Rank of the Transfer Matrix in 1-D Mirrored Interferometric Aperture Synthesis [Text] / L. Chen, Z. Rao, Y. Wang, H. Zhou // IEEE Geoscience and Remote Sensing Letters. – 2017. – Vol. 14, no. 9. – P. 1580-1583, DOI: 10.1109/LGRS.2017.2724602.

10. Novel Synthesis of Shared Aperture Antenna Array Exploiting Concurrently Serving Radiators for Individual Functionality [Text] / K. K. Suman, A. Kumar R., J. K. Modi, R. K. Gangwar, V. S. Gangwar // 2020 IEEE International Conference on Electronics, Computing and Communication Technologies. CONECCT. – Bangalore, 2020. – P. 1-3. DOI: 10.1109/CONECCT50063.2020.9198616.

11. Fomalont E. B. Galactic and Extra-Galactic Radio Astronomy [Text] / E. B. Fomalont, M. C. H. Wright. – Berlin : Springer, 1974. – 694 p.

12. A new method of multi-frequency active aperture synthesis for imaging of SAR blind zone under aerospace vehicle [Text] / V. Pavlikov, V. Volosyuk, S. Zhyla, H. N. Van, K. N. Van // 2017 14th International Conference The Experience of Designing and Application of CAD Systems in Microelectronics. CADSM. – Polyana, 2017. – 118-120. DOI: 10.1109/CADSM.2017.7916099.

13. UWB active aperture synthesis radar the oper-

ating principle and development of the radar block diagram [Text] / V. Pavlikov, V. Volosyuk, S. Zhyla, H. N. Van, K. N. Van // 2017 IEEE Microwaves, Radar and Remote Sensing Symposium. MRRS. – Kiev, 2017. – P. 27-30. DOI: 10.1109/MRRS.2017.8075018.

14. Pavlikov, V. V. Algorithm for radiometric imaging by ultrawideband systems of aperture synthesis [Text] / V. V. Pavlikov, Nguen Van Kiem, O. M. Tymoshchuk // IEEE Radar Methods and Systems Workshop. RMSW. – 2016. – P. 103-106. DOI: 10.1109/RMSW.2016.7778561.

15. Волосюк, В. К. Статистическая теория радиотехнических систем дистанционного зондирования и радиолокации [Текст] / В. К. Волосюк, В. Ф. Кравченко. – М. : Физматлит, 2008. – 704 с.

16. Volosyuk, V. K. Direct and Inverse Transformations in Constructing Spectral Patterns of Random Fields [Text] / V. K. Volosyuk // Optoelectronics, Instrumentation and Data Processing. – 1994. – Vol. 1. – P. 37-42.

17. Volosyuk, V. K. Integral Transforms of Processes and Their Spectral-Correlation Characteristics [Text] / V. K. Volosyuk // Electromagnetic Wave & Electronic Systems. – 1997. – Vol. 2, no. 5. – P. 21-29.

18. Volosyuk, V. K Spectral transformations of wideband fields and their Coherence Functions [Text] / V. K. Volosyuk // Radiophysics and quantum electronics. – 1993. – Vol. 36. no. 11. – P. 804-806.

19. Schooneveld, V. C. Image Formation from Coherence Functions in Astronomy [Text] / V. C. Schooneveld. – Berlin : Springer, 1987. – 340 p.

20. Фалькович, С. Е. Оптимальный прием пространственно-временных сигналов в радиоканалах с рассеянием [Текст] / С. Е. Фалькович, В. И. Пономарев, Ю. В. Шкварко. – М. : Радио и связь, 1989. – 296 с.

21. Ishimaru, A. Wave propagation and scattering in random media [Text] / A. Ishimaru. – New York : Academic Press, 1978. – 572 p.

22. Sakalas, M. Design of a wideband, 4 – 42.5 GHz Low Noise Amplifier in 0.25 µm GaAs pHEMT Technology [Text] / M. Sakalas, P. Sakalas // 2020 IEEE BiCMOS and Compound Semiconductor Integrated Circuits and Technology Symposium. BCICTS. – Monterey, 2020. – P. 1-4. DOI: 10.1109/BCICTS48439.2020.9392907.

23. Sewiolo, B. A 30 GHz Variable Gain Amplifier With High Output Voltage Swing for Ultra-Wideband Radar [Text] / B. Sewiolo, G. Fischer, R. Weigel // IEEE Microwave and Wireless Components Letters. – 2009. – Vol. 19. no. 9. – P. 590-592. DOI: 10.1109/LMWC.2009.2027094.

24. Wang, D. A Gm-Compensated 46-101 GHz Broadband Power Amplifier for High-Resolution FMCW Radars [Text] / D. Wang // 2021 IEEE Interna-tional Symposium on Circuits and Systems. ISCAS. – Sevilla, 2021. – P. 1-5. DOI: 10.1109/ISCAS51556.2021.9401773.

25. Ahmed, A. Mixer-First Extremely Wideband 43–97 GHz RX Frontend with Broadband Quadrature Input Matching and Current Mode Transformer-Based Image Rejection for Massive MIMO Applications [Text] / A. Ahmed, M. Huang, H. Wang // 2020 IEEE Custom Integrated Circuits Conference. CICC. – Boston, 2020. – P. 1-4. DOI: 10.1109/CICC48029.2020.9075896.

26. Rachid, E. A. Ultra-wideband: Very simple printed antennas with Windows in K, Ka and Q bands [Text] / E. A. Rachid, R. M. Farha // 2016 IEEE Conference on Antenna Measurements & Applications. CAMA. – Syracuse, 2016. – P. 1-4. DOI: 10.1109/CAMA.2016.7815731.

27. Simulation and analysis of an ultra-wideband TEM horn antenna with ridge [Text] / S. Lin, S. Yu, J. Jiao, C. Yang // 2017 International Symposium on Antennas and Propagation. ISAP. – Phuket, 2017. – P. 1-2. DOI: 10.1109/ISANP.2017.8228996.

28. Moghaddam, S. M. Ultra-wideband millimeter-wave bowtie antenna [Text] / S. M. Moghaddam, J. Yang, A. A. Glazunov // 2017 International Symposium on Antennas and Propagation. ISAP. – Phuket, 2017. – P. 1-2. DOI: 10.1109/ISANP.2017.8228955.

29. 10-GS/s Sample and Hold System for High-Speed Time-Interleaved ADC [Text] / L Zhang, Q. Kuang, M. Chang, D. Zhang // 2018 Eighth International Conference on Instrumentation & Measurement, Computer, Communication and Control. IMCCC. – Harbin, 2018. – P. 705-708. DOI: 10.1109/IMCCC.2018.00152.

30. Genschow, D. Evaluation of a UWB radar interface for low power radar sensors [Text] / D. Genschow, J. Kloas // 2015 European Radar Conference. EuRAD. – Paris, 2015. – P. 321-324. DOI: 10.1109/EuRAD.2015.7346302

31. Djurovic, I. Time-frequency representation enhancement: ap-proach based on image filtering methods [Text] / I. Djurovic, V. Lukin, A. Roenko // Radioelectronic and Computer Systems. – 2016. – no. 4 (78). – P. 4-21.

32. Li, L. Remote Sensing Image Enhancement Based on Nonsubsampled Shearlet Transform and Local Laplacian Filter [Text] / L. Li, Y. Si // 2018 IEEE 3rd International Conference on Image, Vision and Computing. ICIVC. – Chongqing, 2018. – 415-418. DOI: 10.1109/ICIVC.2018.8492906.

33. Analysis of opportunities to improve image denoising efficiency for dct-based filter [Text] / O. N. Zemliachenko, I. G. Ivakhnenko, G. A. Chernova, V. V. Lukin // Radioelectronic and Computer Systems. – 2018. – no. 2(86). – P. 4-12. DOI: 10.32620/reks.2018.2.01.

34. A Denoising algorithm for remote sensing images with impulse noise [Text] / E. S. Chang, C. Hung, W. Liu, J. Yina // 2016 IEEE International Geoscience and Remote Sensing Symposium. IGARSS. – Beijing, 2016. – P. 2905-2908. DOI: 10.1109/IGARSS.2016.7729750.

35. Improved Noisy Image Quality Assessment Using Multilayer Neural Networks [Text] / A. Rubel, O. Rubel, V. Abramova, G. Proskura, V. Lukin // 2019 IEEE 2nd Ukraine Conference on Electrical and Computer Engineering. UKRCON. – Lviv, 2019. – P. 1046-1051. DOI: 10.1109/UKRCON.2019.8879950.

36. Radar/SAR Image Resolution Enhancement via Unifying Descriptive Experiment Design Regularization and Wavelet-Domain Processing [Text] / Y. V. Shkvarko, J. I. Yañez, J. A. Amao, G. D. Martín del Campo // IEEE Geoscience and Remote Sensing Letters. – 2016. – Vol. 13, no. 2. – P. 152-156. DOI: 10.1109/LGRS.2015.2502539.

References (BSI)

1. Pavlikov, V., Volosyuk, V., Zhyla, S., Van, H. N., Van, K. N. A new method of multi-frequency active aperture synthesis for imaging of SAR blind zone under aerospace vehicle. *2017 14th International Conference The Experience of Designing and Application of CAD Systems in Microelectronics (CADSM)*, 2017, pp. 118-120. DOI: 10.1109/CADSM.2017.7916099.

2. Villano, M., Krieger, G. and Moreira, A. Nadir Echo Removal in Synthetic Aperture Radar via Waveform Diversity and Dual-Focus Postprocessing. *IEEE Geoscience and Remote Sensing Letters*, 2018, no. 15(5), pp. 719-723. DOI: 10.1109/LGRS.2018.2808196

3. Torres, R. and Davidson, M. Overview of Copernicus SAR Space Component and its Evolution. *2019 IEEE International Geoscience and Remote Sensing Symposium (IGARSS 2019)*, 2019, pp. 5381-5384. DOI: 10.1109/IGARSS.2019.8899134

4. Morrison, R. L and Phelps, E. B. Radio Astronomy Techniques for Multistatic Radar Imaging and Localization of Space Objects. *2019 International Applied Computational Electromagnetics Society Symposium (ACES)*, 2019, pp. 1-2.

5. Wei, L., Wijnholds, S. J. and Hurley, P. Robust recovery for aperture synthesis imaging. *2017 IEEE International Conference on Image Processing (ICIP)*, 2017, pp. 3570-3574. DOI: 10.1109/ICIP.2017.8296947.

6. Kuzmin, I. A., Merkulova, Z. V., Sheremet, A. Y., Dovgal, T. A. and Chistukhin, V. V. Methods of multiposition radar aperture synthesis. *2017 IEEE Conference of Russian Young Researchers in Electrical and Electronic Engineering (EIConRus)*, 2017, pp. 1247-1248. DOI: 10.1109/EIConRus.2017.7910789.

7. Pavlikov, V. V., Nguyen Van Kiem, Tymoschuk, O. M. Spectral method for the spatio-spectral sensitivity domain filling in aperture synthesis system. *2016 8th International Conference on Ultrawideband and Ultrashort Impulse Signals (UWBUSIS)*, 2016, pp. 124-127. DOI: 10.1109/UWBUSIS.2016.7724167.

8. Drobakhin, O. O., Sherstyuk, G. G., Mamedov, A. G., Tuluk, A. Y. Inverse aperture synthesis in the intermediate zone of radiation for radio image forming by optimal filtration with evolutionary control. *2016 8th International Conference on Ultrawideband and Ultrashort Impulse Signals (UWBUSIS)*, 2016, pp. 109-111. DOI: 10.1109/UWBUSIS.2016.7724163.

9. Chen, L., Rao, Z., Wang, Y., Zhou, H. The Maximum Rank of the Transfer Matrix in 1-D Mirrored Interferometric Aperture Synthesis. *IEEE Geoscience and Remote Sensing Letters*, 2017, vol. 14, no. 9, pp. 1580-1583. DOI: 10.1109/LGRS.2017.2724602

10. Suman, K. K., Kumar, R. A., Modi, J. K., Gangwar, R. K., Gangwar, V. S. Novel Synthesis of Shared Aperture Antenna Array Exploiting Concurrently Serving Radiators for Individual Functionality. *2020 IEEE International Conference on Electronics, Computing and Communication Technologies (CONECCT)*, 2020, pp. 1-3. DOI: 10.1109/CONECCT50063.2020.9198616.

11. Fomalont, E. B., Wright, M. C. H. *Galactic and Extra-Galactic Radio Astronomy*. Berlin, Springer Publ., 1974. 694 p.

12. Pavlikov, V., Volosyuk, V., Zhyla, S., Van, H. N., Van, K. N. A new method of multi-frequency active aperture synthesis for imaging of SAR blind zone under aerospace vehicle. *2017 14th International Conference The Experience of Designing and Application of CAD Systems in Microelectronics (CADSM)*, 2017, pp. 118-120. DOI: 10.1109/CADSM.2017.7916099.

13. Pavlikov, V., Volosyuk, V., Zhyla, S., Nguyen Van Huu, Nguyen Van Kiem. UWB active aperture synthesis radar the operating principle and development of the radar block diagram, *2017 IEEE Microwaves, Radar and Remote Sensing Symposium (MRRS)*, 2017, pp. 27-30. DOI: 10.1109/MRRS.2017.8075018.

14. Pavlikov, V. V., Nguyen Van Kiem, Tymoschuk, O. M. Algorithm for radiometric imaging by ultrawideband systems of aperture synthesis. *2016 IEEE Radar Methods and Systems Workshop (RMSW)*, 2016, pp. 103-106. DOI: 10.1109/RMSW.2016.7778561.

15. Volosyuk, V. K., Kravchenko, V. F. *Statisticheskaya teoriya radiotekhnicheskikh sistem distantsionnogo zondirovaniya i radiolokatsii* [Statistical Theory of Radio-Engineering Systems of Remote Sensing and

Radar]. Moscow, Fizmatlit Publ., 2008. 704 p.

16. Volosyuk, V. K. Direct and Inverse Transformations in Constructing Spectral Patterns of Random Fields. *Optoelectronics, Instrumentation and Data Processing*, 1995, vol. 1, pp. 37–42.

17. Volosyuk, V. K. Integral Transforms of Processes and Their Spectral-Correlation Characteristics. *Electromagnetic Wave & Electronic Systems*, 1997, vol. 2, no. 5, pp. 21-29.

18. Volosyuk, V. K. Spectral transformations of wideband fields and their Coherence Functions. *Radiophysics and quantum electronics*, 1993, vol. 36, no. 11, pp. 804-806.

19. Schooneveld, V. C. *Image Formation from Coherence Functions in Astronomy*. Berlin, Springer Publ., 1987. 340 p.

20. Falkovich, S. Ye., Ponomarev, V. I., Shkvarko, Y. V., *Optimalnyj priem prostranstvenno-vremenny`x signalov v radiokanalax s rasseyaniem* [Optimal reception of space and time signals in radio channels with scattering]. Moscow, Radio i svyaz Pupl., 1989. 296 p.

21. Ishimaru, A. *Wave propagation and scattering in random media*. New York, Academic Press Publ., 1978. 512 p.

22. Sakalas, M., Sakalas, P. Design of a wideband, 4 – 42.5 GHz Low Noise Ampli-fier in 0.25 µm GaAs pHEMT Technology. *2020 IEEE BiCMOS and Compound Semiconductor Integrated Circuits and Technology Symposium (BCICTS)*, 2020, pp. 1-4. DOI: 10.1109/BCICTS48439.2020.9392907.

23. Sewiolo, B., Fischer, G., Weigel, R. A 30 GHz Variable Gain Amplifier With High Output Voltage Swing for Ultra-Wideband Radar. *IEEE Microwave and Wireless Components Letters*, 2009, vol. 19, no. 9, pp. 590-592. DOI: 10.1109/LMWC.2009.2027094.

24. Wang, D. A Gm-Compensated 46-101 GHz Broadband Power Amplifier for High-Resolution FMCW Radars. *2021 IEEE International Symposium on Circuits and Systems (ISCAS)*, 2021, pp. 1-5. DOI: 10.1109/ISCAS51556.2021.9401773.

25. Ahmed, A., Huang, M., Wang, H. Mixer-First Extremely Wideband 43–97 GHz RX Frontend with Broadband Quadrature Input Matching and Current Mode Transformer-Based Image Rejection for Massive MIMO Applications. *2020 IEEE Custom Integrated Circuits Conference (CICC)*, 2020, pp. 1-4. DOI: 10.1109/CICC48029.2020.9075896.

26. Rachid, E. A., Farha, R. M. Ultra-wideband: Very simple printed antennas with Windows in K, Ka and Q bands. *2016 IEEE Conference on Antenna Measurements & Applications (CAMA)*, 2016, pp. 1-4. DOI: 10.1109/CAMA.2016.7815731.

27. Lin, S., Yu, S., Jiao, J., Yang, C. Simulation and analysis of an ultra-wideband TEM horn antenna with ridge. *2017 International Symposium on Antennas and Propagation (ISAP)*, 2017, pp. 1-2. DOI: 10.1109/ISANP.2017.8228996.

28. Moghaddam, S. M., Yang, J., Glazunov, A. A. Ultra-wideband millimeter-wave bowtie antenna. *2017 International Symposium on Antennas and Propagation (ISAP)*, 2017, pp. 1-2. DOI: 10.1109/ISANP.2017.8228955.

29. Zhang, L., Kuang, Q., Chang, M., Zhang, D. 10-GS/s Sample and Hold System for High-Speed Time-Interleaved ADC. *2018 Eighth International Conference on Instrumentation & Measurement, Computer, Communication and Control (IMCCC)*, 2018, pp. 705-708. DOI: 10.1109/IMCCC.2018.00152.

30. Genschow, D., Kloas, J. Evaluation of a UWB radar interface for low power radar sensors. *2015 European Radar Conference (EuRAD)*, 2015, pp. 321-324. DOI: 10.1109/EuRAD.2015.7346302

31. Djurovic, I., Lukin, V., Roenko, A. Time-frequency representation enhancement: approach based on image filtering methods. *Radioelectronic and Computer Systems*, 2016, no. 4(78), pp. 4-21.

32. Li, L., Si, Y. Remote Sensing Image Enhancement Based on Nonsub-sampled Shearlet Transform and Local Laplacian Filter. *International Conference on Image, Vision and Computing (ICIVC)*, 2018, pp. 415-418. DOI: 10.1109/ICIVC.2018.8492906.

33. Zemliachenko, O. N., Ivakhnenko, I. G., Chernova, G.A., Lukin, V. V. Analysis of opportunities to improve image denoising efficiency for dct-based filter. *Radioelectronic and Computer Systems*, 2018, no. 2(86), pp. 4-12. DOI: 10.32620/reks.2018.2.01.

34. Chang, E. S., Hung, C., Liu, W., Yina, J. A Denoising algorithm for remote sensing images with impulse noise. *2016 IEEE International Geoscience and Remote Sensing Symposium (IGARSS)*, 2016, pp. 2905-2908. DOI: 10.1109/IGARSS.2016.7729750.

35. Rubel, A., Rubel, O., Abramova, V., Proskura, G., Lukin, V. Improved Noisy Image Quality Assessment Using Multilayer Neural Networks. *2019 IEEE 2nd Ukraine Conference on Electrical and Computer Engineering (UKRCON)*, 2019, pp. 1046-1051. DOI: 10.1109/UKRCON.2019.8879950.

36. Shkvarko, Y. V., Yañez, J. I., Amao, J. A., Martín del Campo, G. D. Radar/SAR Image Resolution Enhancement via Unifying Descriptive Experiment Design Regularization and Wavelet-Domain Processing. *IEEE Geoscience and Remote Sensing Letters*, 2016, vol. 13, no. 2, pp. 152-156. DOI: 10.1109/LGRS.2015.2502539.

МАТЕМАТИЧНИЙ ОПИС ПРОЦЕСІВ ФОРМУВАННЯ ЗОБРАЖЕНЬ В НАДШИРОКОСМУГОВИХ СИСТЕМАХ АКТИВНОГО АПЕРТУРНОГО СИНТЕЗУ З ВИКОРИСТАННЯМ СТОХАСТИЧНИХ ЗОНДУЮЧИХ СИГНАЛІВ

В. К. Волосюк, С. С. Жила, В. В. Павліков, Е. О. Церне,
А. Д. Собколов, О. О. Шматко, К. Г. Бєлоусов

Наводяться математичні моделі полів стохастичних надширокосмугових сигналів, необхідних для вирішення завдань апертурного синтезу зображень методами активної радіолокації. Обґрунтовано доцільність застосування в цих завданнях V-перетворень, ефективність яких вже доведена для математичного опису надширокосмугових просторово-часових полів у методах пасивної та активної радіолокації, а також дистанційного зондування, що застосовуються для вирішення завдань радіоастрономії, медицини, навігації тощо. Використовуючи сучасні методи математичного аналізу та теорії синтезу надширокосмугових систем, досліджено фізичну сутність радіозображень, що одержуються за допомогою алгоритмів когерентної та некогерентної обробки сигналів. Відповідно до цих алгоритмів запропоновано розділити зображення на когерентні та некогерентні. До когерентних зображень відносять такі, в яких окремо фіксуються їх амплітуда та фаза. У разі некогерентного зображення фіксується лише його амплітуда (потужність чи пов'язана з нею характеристика). Для коректного опису структури радіозображень, що одержуються, запроваджено нові поняття спектральної густини комплексної функції просторової когерентності (СГКФПК) та спектральної густини просторової автокореляційної функції амплітудно-фазового розподілу (СГПАКФ АФР). Застосування даних функцій доцільне і принципово необхідне при вирішенні завдань апертурного синтезу з використанням стохастичних надширокосмугових сигналів. Дано математичний опис структур, що одержуються при апертурному синтезі радіозображень. Водночас дослідження проведені для загального випадку використання континуальної (ідеалізованої) апертури і для застосування антенної системи з просторово рознесеними приймальними елементами. Виконано імітаційне моделювання синтезованого евристичним шляхом алгоритму побудови некогерентних радіозображень. Обґрунтовано можливість застосування антенних решіток та синтезованих алгоритмів апертурного синтезу для вирішення завдань формування зображень у мертвій зоні огляду, що розташовується безпосередньо під літальним апаратом (при кутах зондування, близьких до вертикальних).

Ключові слова: активний апертурний синтез; формування зображень за допомогою радару; V-перетворення.

МАТЕМАТИЧЕСКОЕ ОПИСАНИЕ ПРОЦЕССОВ ФОРМИРОВАНИЯ ИЗОБРАЖЕНИЙ В СВЕРХШИРОКОПОЛОСНЫХ СИСТЕМАХ АКТИВНОГО АПЕРТУРНОГО СИНТЕЗА С ИСПОЛЬЗОВАНИЕМ СТОХАСТИЧЕСКИХ ЗОНДИРУЮЩИХ СИГНАЛОВ

В. К. Волосюк, С. С. Жила, В. В. Павликов, Э. А. Цернэ,
А. Д. Собколов, А. А. Шматко, К. Г. Белоусов

Приводятся математические модели полей стохастических сверхширокополосных сигналов, необходимые для решения задач апертурного синтеза изображений методами активной радиолокации. Обоснована целесообразность применения в этих задачах V-преобразований, эффективность которых уже доказана для математического описания сверхширокополосных пространственно-временных полей в методах пассивной и активной радиолокации, а также дистанционного зондирования, применяемых для решения задач радиоастрономии, медицины, навигации и др. Используя современные методы математического анализа и теории синтеза сверхширокополосных систем, исследована физическая сущность радиоизображений, получаемых с помощью алгоритмов когерентной и некогерентной обработки сигналов. Соответственно этим алгоритмам предложено разделить изображения на когерентные и некогерентные. К когерентным изображениям относят такие, в которых раздельно фиксируются его амплитуда и фаза. В случае некогерентного изображения фиксируется только его амплитуда (мощность или связанная с ней характеристика). Для корректного описания структуры получаемых радиоизображений введены новые понятия спектральной плотности комплексной функции пространственной когерентности (СПКФПК) и спектральной плотности пространственной автокорреляционной функции амплитудно-фазового распределения (СППАКФ АФР). Применение данных функций целесообразно и принципиально необходимо при решении задач апертурного синтеза с использованием стохастических сверхширокополосных сигналов. Дано математическое описание структур, получаемых при апертурном синтезе радиоизображений. При этом исследования проведены для общего случая использования континуальной (идеализированной) апертуры, и для применения антенной системы с пространственно разнесёнными приёмными элементами. Выполнено имитационное моделирование синтезированно-

го эвристическим путем алгоритма построения некогерентных радиоизображений. Обоснована возможность применения антенных решеток и синтезированных алгоритмов апертурного синтеза для решения задач формирования изображений в мертвой зоне обзора, располагаемой непосредственно под летательным аппаратом (при углах зондирования близких к вертикальным).

Ключевые слова: Активный апертурный синтез; построение изображений с помощью радара; V-преобразования.

Волосюк Валерій Костянтинович – д-р техн. наук, проф., проф. каф. аерокосмічних радіоелектронних систем, Національний аерокосмічний університет ім. М. Є. Жуковського «Харківський авіаційний інститут», Харків, Україна.

Жила Семен Сергійович – д-р техн. наук, зав. каф. аерокосмічних радіоелектронних систем, Національний аерокосмічний університет ім. М. Є. Жуковського «Харківський авіаційний інститут», Харків, Україна.

Павліков Володимир Володимирович – д-р техн. наук, проф., проректор з наукової роботи, Національний аерокосмічний університет ім. М. Є. Жуковського «Харківський авіаційний інститут», Харків, Україна.

Церне Едуард Олексійович – асист. каф. аерокосмічних радіоелектронних систем, Національний аерокосмічний університет ім. М. Є. Жуковського «Харківський авіаційний інститут», Харків, Україна.

Собколов Антон Дмитрович – наук. співроб. каф. аерокосмічних радіоелектронних систем, Національний аерокосмічний університет ім. М. Є. Жуковського «Харківський авіаційний інститут», Харків, Україна.

Шматко Олександр Олександрович – канд. техн. наук, докторант каф. аерокосмічних радіоелектронних систем, Національний аерокосмічний університет ім. М. Є. Жуковського «Харківський авіаційний інститут», Харків, Україна.

Бєлоусов Костянтин Георгійович – головний конструктор і начальник проектно-конструкторського бюро космічних апаратів, систем вимірювань і телекомунікацій КБ Південне, Дніпро, Україна.

Valeriy Volosyuk – D.Sc. in Radioengineering, Professor of Department of Aerospace Radio-electronic Systems, National Aerospace University "Kharkiv Aviation Institute", Kharkiv, Ukraine,
e-mail: v.volosyuk@khai.edu, ORCID: 0000-0002-1442-6235, ResearcherID: A-2021-2019.

Simeon Zhyla – D.Sc. in Radioengineering, Head of Department of Aerospace Radio-electronic Systems, National Aerospace University "Kharkiv Aviation Institute", Kharkiv, Ukraine,
e-mail: s.zhyla@khai.edu, ORCID: 0000-0003-2989-8988, Scopus Author ID: 35106469000.

Volodimir Pavlikov – D.Sc. in Radioengineering, Vise rector for Science, National Aerospace University "Kharkiv Aviation Institute", Kharkiv, Ukraine,
e-mail: v.pavlikov@khai.edu, ORCID: 0000-0002-6370-1758, Scopus Author ID: 23397933100.

Eduard Tserne – Assistant of Department of Aerospace Radio-electronic Systems, National Aerospace University "Kharkiv Aviation Institute", Kharkiv, Ukraine,
e-mail: e.tserne@khai.edu, ORCID: 0000-0003-0709-2238, Scopus Author ID:57218704755.

Anton Sobkolov – Researcher of Department of Aerospace Radio-electronic Systems, National Aerospace University "Kharkiv Aviation Institute", Kharkiv, Ukraine,
e-mail: a.sobkolov@khai.edu, ORCID: 0000-0001-9356-4187, Scopus Author ID: 57192199954.

Olexandr Shmatko – PhD in Radioengineering, doctoral student of Department of Aerospace Radio-electronic Systems, National Aerospace University "Kharkiv Aviation Institute", Kharkiv, Ukraine,
e-mail: o.shmatko@khai.edu, ORCID: 0000-0002-3236-0735.

Konstantin Belousov – Chief Designer, Head of Spacecraft, Measuring Systems and Telecommunications in Yuzhnoye SDO, Dnipro, Ukraine,
e-mail: info@yuzhnoye.com, ORCID: 0000-0002-6436-3359.